

# Mass Diffusion and Thermal Diffusivity of the Decane-pentane Mixture Under High Pressure as a Ground-based Study for SCCO Project

Ion Lizarraga<sup>1</sup> · Cédric Giraudet<sup>2</sup> · Fabrizio Croccolo<sup>2</sup> · M. Mounir Bou-Ali<sup>1</sup> · Henri Bataller<sup>2</sup>

Received: 30 January 2016 / Accepted: 27 May 2016 / Published online: 16 June 2016  
© Springer Science+Business Media Dordrecht 2016

**Abstract** Thermodiffusion experiments on isomassic binary mixture of decane and pentane in the liquid phase have been performed between 25 °C and 50 °C and for pressures from 1MPa until 20MPa. By dynamic analysis of the light scattered by concentration non-equilibrium fluctuations in the binary mixture we obtained the mass diffusion coefficients of the mixture at each temperature and pressure. For the first time we were able to apply similar analysis to thermal fluctuations thus getting a simultaneous measurement of the thermal diffusivity coefficient. While mass diffusion coefficients decrease linearly with the pressure, thermal diffusivity coefficients increase linearly. In principle the proposed method can be used also for measuring the Soret coefficients at the same time. However, for the present mixture the intensity of the optical signal is limited by the optical contrast factor. This affects our capability of providing a reliable estimate of the Soret coefficient

by means of dynamic Shadowgraph. Therefore the mass diffusion coefficients measurements would need to be combined with independent measurements of the thermodiffusion coefficients, e.g. thermogravitational column, to provide Soret coefficients. The obtained values constitute the on-ground reference measurements for one of the mixture studied in the frame of the project SCCO-SJ10, which aims to measure the Soret coefficients of multicomponents mixtures under reservoir conditions. Microgravity experiments will be performed on the Chinese satellite SJ10 launched in April 2016.

**Keywords** Mass diffusion · Thermal diffusivity · Decane-pentane mixture · Non-equilibrium fluctuations · High pressure · SCCO · SJ10

## Introduction

The precise modelling of the distribution of chemical species in oil and gas reservoirs remains a topical issue for the oil industry, especially now that the reserves of fossil fuels are getting more difficult to extract. It is known that not only gravitational segregation, but also thermodiffusion due to geothermal gradients, are two physical phenomena determining the vertical distribution of species in hydrocarbon reservoirs on Earth (Lira-Galeana et al. 1994, Høier et al. 2001, Ghorayeb et al. 2003, Montel et al. 2007). Thermodiffusion, or Soret effect, is a phenomenon that couples heat and mass fluxes (de Groot and Mazur 1984) and can also lead to convective unstable conditions in particular cases (Galliero et al. 2009). The contribution of thermodiffusion is difficult to quantify, mainly due to a lack of

---

This article belongs to the Topical Collection: Advances in Gravity-related Phenomena in Biological, Chemical and Physical Systems

Guest Editors: Valentina Shevtsova, Ruth Hemmersbach

---

✉ Henri Bataller  
henri.bataller@univ-pau.fr

<sup>1</sup> MGEP Mondragon Goi Eskola Politeknikoa, Mechanical and Industrial Manufacturing Department, Loramendi 4 Apdo. 23, 20500 Mondragon, Spain

<sup>2</sup> Laboratoire des Fluides Complexes et leurs Réservoirs, UMR-5150, Université de Pau et des Pays de l'Adour, 1 Allée du Parc Montaury, Anglet, France

experimental data as well as accurate modeling for multi-component mixtures. Although noticeable progresses have been made during the last twenty years, (Assael et al., 2014 and references therein) especially on ternary mixtures both theoretically (Firoozabadi et al., 2000; Kempers, 2001; Galliero et al., 2003) and experimentally (Leahy-Dios et al., 2005; Larrañaga et al., 2015; Gebhardt et al., 2015), more work is necessary. Micro-gravity experiments, to avoid gravity-induced convection, are one possible way to provide further data on thermodiffusion in multicomponent mixtures (Georis et al., 1998; Van Vaerenbergh et al., 2009; Touzet et al., 2011; Bou-Ali et al., 2015). The Soret Coefficients in Crude Oil (SCCO) project aims at producing values of Soret coefficients of mixture of petroleum interest and in reservoirs conditions. In a first phase carried out in 2007 microgravity experiments were performed on board the Russian satellite FOTON-M3. One binary, two ternaries and one quaternary mixtures were studied (Van Vaerenbergh et al., 2009; Srinivasan et al., 2009; Touzet et al., 2011). The measurements were compared with molecular dynamics simulations and with theoretical calculations based on the Thermodynamics of Irreversible Processes. However, the conclusions were incomplete because of difficulties encountered during post flight analysis at the laboratories (Touzet et al., 2011). Now, on the occasion of the China Sea well explorations, a second phase of the SCCO space experiment has been scheduled. The thermodiffusion behaviour of the binary mixture decane-pentane, the ternary mixture decane-heptane-pentane and the quaternary mixture decane-heptane-pentane-methane, at two pressures and at 50 °C, will be studied on-board the Shijian-10 (SJ-10) Chinese satellite during 2016 (Galliero et al., 2016). To assure the success of this new mission, both validating ground measurements and numerical simulations have been planned. In this paper we present results on the isomassic binary mixture decane-pentane based on the measurement of non-equilibrium (NE) fluctuations.

In general, from the analysis of the dynamics of concentration NE fluctuations by light-scattering it is possible to measure the fluid transport properties coefficients, including the mass diffusion and Soret coefficients, as demonstrated for binary mixtures (Croccolo et al., 2012, 2014). The technique has been adapted to high pressure (Giraudet et al., 2014). In this work we extend the technique to the analysis of thermal fluctuations thus including the possibility of measuring the thermal diffusivity coefficient of the mixture. Conversely, due to the limited amplitude of the optical signal obtained for this system, we were not able here to measure the Soret coefficient.

The remainder of the paper is organized as follows: Section “[Methodology](#)” reports the methodology, in Section “[Results and Discussion](#)” we provide results and discussion, and in Section “[Conclusions](#)” conclusions are drawn.

## Methodology

**Theoretical background** In a homogeneous multicomponent mixture a temperature gradient induces heat transfer as well as segregation of the components along the temperature gradient by means of the Soret effect (de Groot and Mazur, 1984). The segregation induces then Fickian diffusion and the combination of the two phenomena results in a steady concentration gradient which is convection-free only in microgravity conditions or in particular cases on ground. A thermodiffusion experiment on ground is typically performed by applying a stabilizing thermal gradient to a multicomponent fluid mixture, thus obtaining a superposition of the mentioned phenomena. Even if there is no total mass flux in the steady state, thermal and concentration NE fluctuations are always present. NE fluctuations are strictly related to the transport properties of the fluid. That is why from NE fluctuations analysis one can determine in principle all transport coefficients, like viscosity, thermal diffusivity and solutal diffusion and thermodiffusion coefficients. A detailed description of the theory of NE fluctuations can be found in the book by Ortiz de Zárate and Sengers (2006). Here we briefly recall the essential equations that will be used in the following.

In a binary mixture, the temporal correlation function of NE concentration fluctuations induced by the Soret effect is expected to be a single exponential decay for all wave vectors, with time constants  $\tau_S(q)$  varying as a function of the wave vector  $q$ . For wave vectors much larger than a characteristic value  $q_s^*$ , the decay time is the solutal diffusive one:

$$\tau_S(q) = 1/(Dq^2), \quad (1)$$

where  $D$  is the mass diffusion coefficient. NE thermal fluctuations are faster and overlap to the solutal ones. For wave vectors larger than a thermal characteristic wave vector  $q_T^*$ , the decay time is the thermal diffusive one:

$$\tau_T(q) = 1/(\kappa q^2), \quad (2)$$

where  $\kappa$  is the thermal diffusivity coefficient.

**Experimental set-up** Our thermodiffusion cell (Fig. 1 of Giraudet et al., 2014) is specifically designed for applying a vertical temperature gradient with excellent thermal homogeneity and stability to a horizontal slab of a multicomponent fluid under high pressure while providing vertical optical access to a central area of the cell. The cell core consists of a stainless steel annulus of internal/external diameter 30/75mm with high pressure inlet and outlet at its opposite sides. This part accommodates Teflon® -coated Viton® O-rings for sealing, and square sapphire plates kept at a distance  $L = 5\text{mm}$  by the annulus itself, thus defining the sample thickness. In order to minimize the contact between

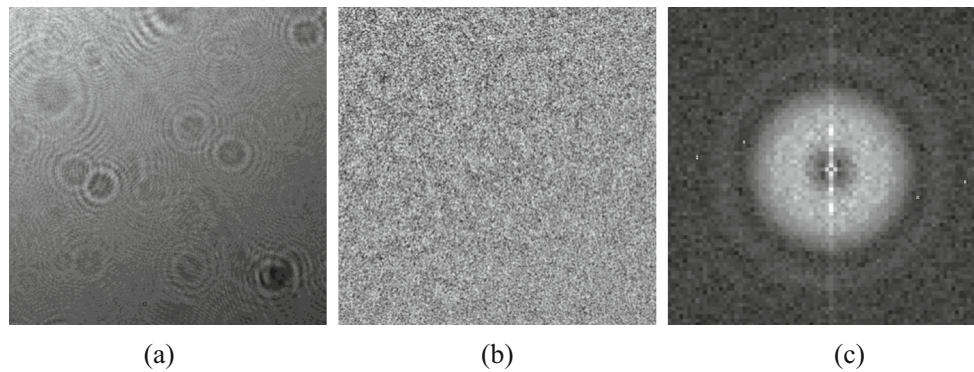


**Fig. 1** Results of a near field scattering experiment (shadowgraph layout) on the isomassic binary of decane and pentane stressed by a thermal gradient ( $T_{mean} = 50$  °C,  $P = 20$  MPa,  $\Delta T = 30$  °C ). (a)  $768 \times 768$  pix<sup>2</sup> near field image of the sample,  $I(\vec{x}, t)$  (b) image

difference,  $\Delta I(\vec{x}, \Delta t) = I(\vec{x}, t + \Delta t) - I(\vec{x}, t)$ , having a correlation time of  $\Delta t = 0.35$  s and (c) 2D Fast Fourier Transform squared  $|I(\vec{q}, t + \Delta t) - I(\vec{q}, t)|^2$  of (b)

the liquid sample and the conductive metal a Teflon annulus (internal/external diameter 19.8/30mm) with two thin holes (diameter 1mm) for inlet/outlet of the fluid has been inserted in the inner part of the stainless annulus zone.

The external sides of the sapphire windows are in thermal contact with two aluminium plates with a central circular aperture ( $d = 13$ mm), where two thermistors (Wavelength Electronics, TCS651) are installed to monitor the sapphire temperatures. External to the aluminium plates, two Peltier elements (Kryotherm, TB-109-1.4-1.5 CH) with central circular aperture ( $d = 13$ mm) provide/remove the heat necessary to maintain the set-point temperature as driven by two temperature controllers (Wavelength Electronics, LFI-3751) maintaining the temperature of the internal side of each Peltier device with a stability better than 1mK RMS over 1 day. Finally, external to the Peltier elements, two aluminium plates are flushed with water coming from a thermostatic bath (Huber, ministat 125) to remove the excess heat of the Peltiers.

Experiments have been performed with the isomassic binary mixture of decane (Sigma-Aldrich,  $\geq 99$  %) and pentane (Sigma-Aldrich,  $\geq 99$  %). Components were used without further purification. The mixture is prepared in a bottle by weighting on a balance (Sartorius, TE313S, resolution  $10^{-2}$ g/200g) first the decane and then the pentane. The bottle is carefully closed by cover with Teflon sealing. Error in mass fraction is estimated less than  $\pm 0.0001$ .

The filling system consists of: a rotary vacuum pump able to evacuate most of the air from the cell before filling operations down to a residual pressure of about 10Pa; a fluid vessel at atmospheric pressure; a manual volumetric pump and a number of valves to facilitate the procedure. Briefly, after a low vacuum is made inside the cell, the mixture to be studied is transferred to the cell by acting on the volumetric pump. Visual check allows avoiding bubbles during the injection procedure. After that, the cell is abundantly

fluxed with the fluid mixture. At the end of the procedure a valve is closed and the volumetric pump is operated to modify the liquid pressure within the cell. A manometer (Keller, PAA-33X, pressure range: 0.1÷100MPa, precision  $\pm 0.04$ MPa) is connected between the volumetric pump and the cell to measure the pressure of the fluid mixture. A second identical manometer is connected to the outlet of the cell. The manometer signals are transferred using an acquisition card (National Instruments, NI 9215) interfaced to a computer.

We perform our experiments by imposing a difference of temperature  $\Delta T$  on the horizontally positioned thin cell, previously filled with the homogenous fluid mixture.

In order to investigate NE fluctuations, it is common to use a scattering in the near field technique as the Shadowgraph (Wu et al. 1995), for which the physical optics treatment was given by Trainoff and Cannell (2002) and Croccolo and Brogioli (2011). The shadowgraph optical setup involves a low coherence light source (Super Lumen, SLD-MS-261-MP2-SM,  $\lambda = 675 \pm 13$ nm) that illuminates the bottom of the cell through a single-mode fiber. The diverging beam exiting from the fiber end is collimated by an achromatic doublet lens ( $f = 150$ mm,  $\varphi = 50.8$ mm) and then passes through a linear film polarizer. In combination with a second linear polarizer after the cell the latter allows us to adapt the average light intensity.

The detection plane is located at about  $z = 95$ mm from the sample plane. As a sensor, we use a charge coupled device (AVT, PIKE-F421B) with  $2048 \times 2048$  square pixels each of size  $7.4 \times 7.4 \mu\text{m}^2$  and a dynamic range of 14-bit. Images were cropped within a  $768 \times 768$  pix<sup>2</sup> in order to reach the maximum acquisition frame rate of the camera of about 30Hz.

**Dynamic near-field imaging** Images acquired by means of a near-field scattering setup consist of an intensity map

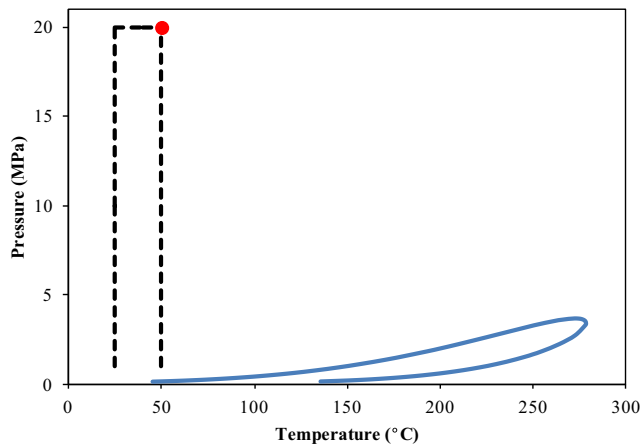


**Fig. 2** Phase diagram of the isomassic binary mixture decane-pentane: the continuous line represents the biphasic envelop. The dashed lines represent the values of pressure and temperature investigated for the reported thermodiffusion experiments. The red point indicates the thermodynamic conditions of the thermodiffusion experiment shown in Figs. 1, 3 and 4 ( $T_{mean} = 50\text{ }^{\circ}\text{C}$ ,  $P = 20\text{ MPa}$ )

$I(\vec{x}, t)$  generated by the interference on the CCD plane between the portion of the incident beam that has passed undisturbed through the sample and the beams scattered by refractive index fluctuations occurring within the sample (Trainoff and Cannell, 2002; Crococo and Brogioli, 2011). Statistical analysis involving fast Fourier transforms provides accurate measurements of the intensity  $I_s(\vec{q}, t)$  of light scattered at each wave vector  $\vec{q}$  grabbed by the optical setup and for all the times  $t$  of the acquisition sequence. Different setups show different responses to the acquired signal as a function of the wave number  $q$ , which is described by the so-called transfer function  $T(q)$ .

Details of the quantitative dynamic analysis can be found elsewhere (Crococo et al., 2006a; Crococo et al., 2006b; Crococo et al., 2007; Cerchiari et al., 2012). Here we just recall that the quantity directly obtained from the experiments is the so-called structure function  $C_m(q, \Delta t) =$

$\langle |\Delta I_m(q, \Delta t)|^2 \rangle$ , that is obtained by averaging (over all available times  $t$  in each image dataset and over the wave vector  $\vec{q}$  azimuthal angle) the individual spatial Fourier transforms of the shadowgraph image differences, like the one shown in the example of Fig. 1. This experimental structure function is theoretically related to the temporal correlation function of NE composition fluctuations, also called intermediate scattering function (ISF), by:

$$C_m(q, \Delta t) = 2 \{ S(q) T(q) [1 - ISF(q, \Delta t)] + B(q) \}, \quad (3)$$

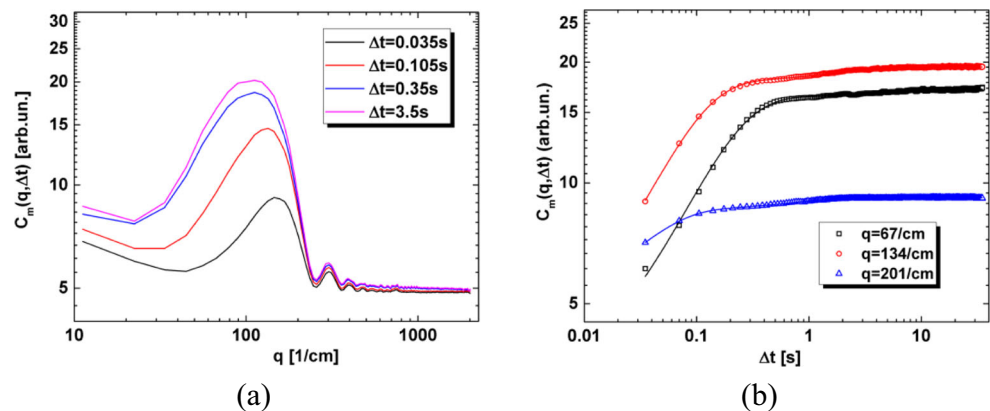
with  $ISF(q, 0) = 1$ . In Eq. 3,  $S(q)$  is the static power spectrum of the sample,  $T(q)$  is the optical transfer function and  $B(q)$  the background noise of the measurement. It is implicitly assumed in Eq. 3 that the linear response of the CCD detector and any other electronic or electromagnetic proportionality parameters are aggregated inside  $T(q)$  and/or  $B(q)$ .

## Results and Discussion

**Thermodynamic conditions** To determine the thermodynamic conditions of the study, we have calculated, with TOTAL S.A. company BEST software, the biphasic envelop and critical coordinates of the isomassic binary mixture of decane and pentane. For a given pressure  $P$  and a given temperature  $T$ , the software calculates the possible molar volumes  $v$  from the PPR78 equation of state (Peng and Robinson, 1976). In Fig. 2 we report the calculated biphasic envelop.

In Fig. 2 the dashed line represents the values of pressure and temperature investigated for the present thermodiffusion experiments, the temperature of  $50\text{ }^{\circ}\text{C}$  being imposed by the microgravity experimental conditions of the SCCO project, and the temperature of  $25\text{ }^{\circ}\text{C}$  being selected as the experimental data references for mass diffusion coefficients

**Fig. 3** Experimental structure function  $C_m(q, \Delta t)$  (a) as a function of the wave vector  $q$  for different correlation times  $\Delta t$  and (b) as a function of the correlation time  $\Delta t$  for different wave vectors  $q$  ( $T_{mean} = 50\text{ }^{\circ}\text{C}$ ,  $P = 20\text{ MPa}$ ,  $\Delta T = 30\text{ }^{\circ}\text{C}$ )





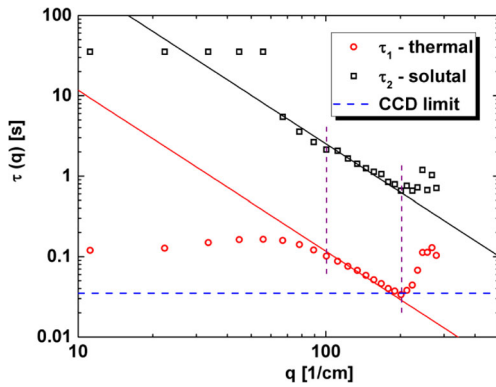


**Fig. 4** Experimental decay times of NE fluctuations as obtained by fitting through Eqs. 3 and 4, as a function of the wave number  $q$ .  $\circ$ : fast mode,  $\square$ : slow mode ( $T_{mean} = 50^\circ\text{C}$ ,  $P = 20\text{MPa}$ ,  $\Delta T = 30^\circ\text{C}$ ). The black solid line represents the theoretical relaxation times  $1/Dq^2$  of Eq. 1 and the red solid line represents the theoretical relaxation times  $1/\kappa q^2$  of Eq. 2

only exist at this temperature. Initially, a temperature difference of  $20^\circ\text{C}$  was applied to the system. To increase the optical signal, which remains low as revealed by Fig. 1b-c, we applied a temperature difference of  $30^\circ\text{C}$ . In all the investigated conditions the mixture was in its liquid state, even at low pressure and for temperature differences of  $\Delta T = 20$  and  $30^\circ\text{C}$ . The red point in Fig. 2 indicates the thermodynamic conditions of the thermodiffusion experiment shown in Figs. 1, 3 and 4 ( $T_{mean} = 50^\circ\text{C}$ ,  $P = 20\text{MPa}$ ).

**Structure function** At each investigated temperature  $T$  and pressure  $P$ , 10 different image acquisition runs have been performed with a delay time  $dt_{min} = 35\text{ms}$  between two consecutive images. Each set, containing 2000 images, has then been processed on a dedicated PC by means of a custom-made CUDA/C++ software (Cerchiarì et al., 2012), in order to perform a fast parallel processing of the images to obtain the structure functions  $C_m(q, \Delta t)$ , for all

the wave numbers and for all the correlation times accessible within the image datasets. In each experiment the temperature gradient is applied via two distinct temperature controllers, so that a linear temperature gradient sets up in some tens of seconds. The image acquisition is started about five hours later, to be sure that the concentration gradient due to the Soret effect is fully developed within the cell.

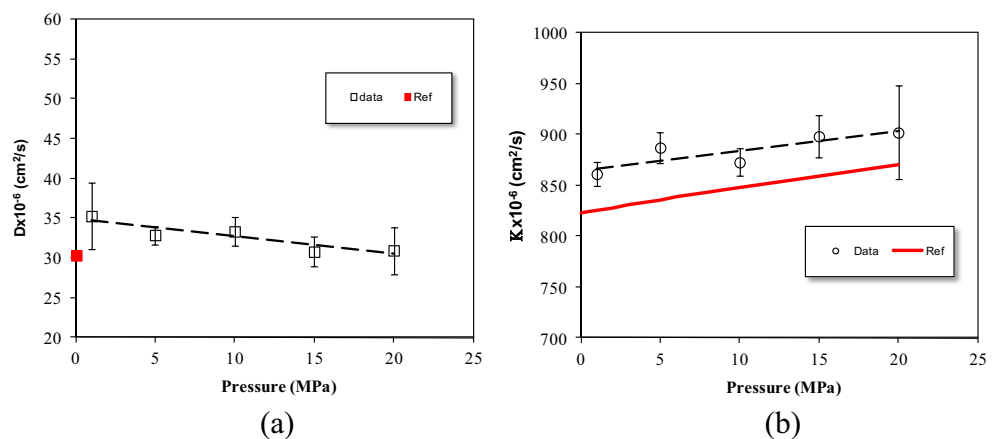
In Fig. 3 we present the mean structure function  $C_m(q, \Delta t)$  of the 10 runs a) as a function of the wave number for different correlation times and b) as a function of the correlation time for different wave numbers, for mean temperature  $T_{mean} = 50^\circ\text{C}$ , pressure  $P = 20\text{MPa}$  and a difference of temperature  $\Delta T = 30^\circ\text{C}$ . The oscillatory behavior shown in Fig. 3a is due to the optical transfer function  $T(q)$  (see Eq. 3). It is typical of shadowgraph experiments and it corresponds to the ring pattern shown in Fig. 1c.

Figure 3a shows that for wave numbers  $q > 400\text{cm}^{-1}$ , the signal is completely lost in the background noise. For intermediate wave numbers, Fig. 3b shows that the time dependence of the structure function cannot be totally assumed mono-exponential, as it is visible for wave numbers  $q = 134\text{cm}^{-1}$  and  $201\text{cm}^{-1}$ . To account for the solutal relaxation mode plus the thermal relaxation mode, we therefore decided to perform a quantitative analysis of the experimental structure functions by modeling the ISF as a double exponential decay, namely:

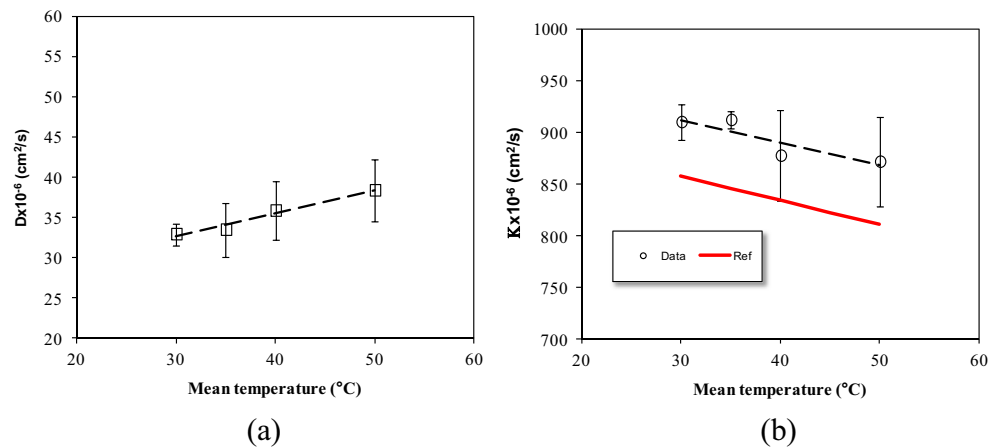
$$ISF(q, \Delta t) = a \exp\left(-\frac{\Delta t}{\tau_1(q)}\right) + (1 - a) \exp\left(-\frac{\Delta t}{\tau_2(q)}\right), \tag{4}$$

where  $\tau_1$  and  $\tau_2$  are two relaxation times. Hence, we performed fittings of the experimental  $C_m(q, \Delta t)$  as a function of  $\Delta t$  (see Fig. 3b) by substituting Eq. 4 into Eq. 3 and adopting as fitting parameters: the product  $S(q)T(q)$ , the background  $B(q)$ , the relative amplitude  $a$ , and the two decay times,  $\tau_1$  and  $\tau_2$ . For the fitting procedure we used

**Fig. 5** Mass diffusion  $D$  and thermal diffusivity  $\kappa$  coefficients as a function of the pressure at  $T_{mean} = 25^\circ\text{C}$  and for a temperature difference of  $\Delta T = 20^\circ\text{C}$



**Fig. 6** Mass diffusion  $D$  and thermal diffusivity  $\kappa$  coefficients as a function of the mean temperature at  $P=20\text{MPa}$  and for a temperature difference of  $\Delta T = 30^\circ\text{C}$



a Levenberg-Marquardt Non-Linear Least Square fitting algorithm.

In Fig. 4 we show the two decay times obtained from modeling the *ISF* by Eq. 4, as a function of the wave number. The horizontal dashed blue line corresponds to  $dt_{\min} = 35\text{ms}$ , which is the physical limit of our experimental recording equipment.

Intuitively, we assumed that the fastest mode was associated with a thermal mode and the slowest to a solutal mode.

In the range of wave numbers  $100\text{cm}^{-1} \leq q \leq 200\text{cm}^{-1}$  (vertical dotted lines are plotted in Fig. 4 to guide the reader) the slowest mode was fitted with Eq. 1 using  $D$  as free parameter and the fastest was fitted with Eq. 2 using  $\kappa$  as free parameter. The results of the adjustments are reported by continuous lines in Fig. 4. For example, referring to the conditions of Fig. 4 ( $P = 20\text{MPa}$ ,  $T_{\text{mean}} = 50^\circ\text{C}$ ) the two values obtained by fitting are  $D = (38 \pm 4) \times 10^{-6} \text{ cm}^2/\text{s}$  and  $\kappa = (870 \pm 40) \times 10^{-6} \text{ cm}^2/\text{s}$ . Uncertainties are the average of the deviations respect to the mean value of the 10 measurements.

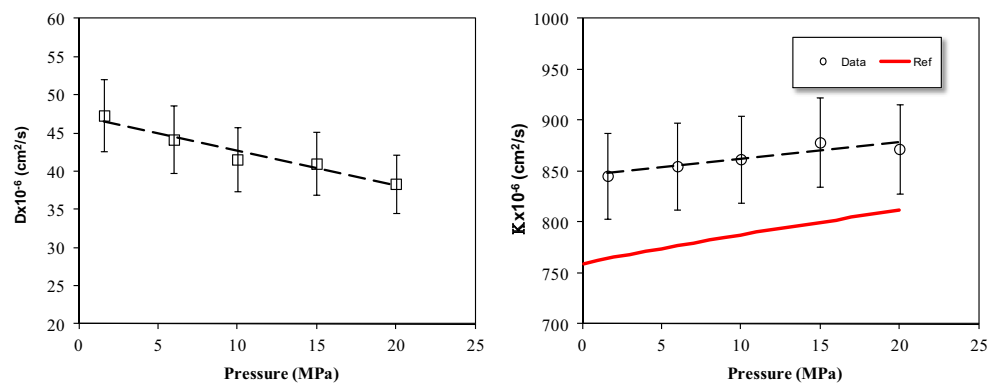
**Mass diffusion and thermal diffusivity coefficients** In Fig. 5 we report the values of mass diffusion and thermal diffusivity coefficients as a function of the pressure obtained

for the isomassic binary mixture of decane and pentane, at  $T_{\text{mean}} = 25^\circ\text{C}$  and for a temperature difference  $\Delta T = 20^\circ\text{C}$ .

We found only one reference value of the mass diffusion coefficients at atmospheric pressure (Alonso De Mezquia et al., 2012) that we reported in Fig. 5a as a red point. The thermal diffusivity coefficients were compared with values found in NIST data base (NIST website: <http://webbook.nist.gov/chemistry/>) and reported by a red continuous line in Fig. 5b. Our values slightly overestimate reference values. However, over the entire pressure range studied, the relative deviation of the thermal diffusivity coefficients values does not exceed 5%. These results validate our hypothesis for the interpretation of the modes of the measured intermediate scattering function, namely that the fastest mode is the thermal relaxation mode of NE fluctuations and the slowest a mass relaxation mode.

In Fig. 5a we can notice a slight linear decrease in the mass diffusion coefficient with pressure that is consistent with an increase of the viscosity with pressure (mass diffusion coefficient being proportional to the inverse of the viscosity), as it has been shown in Alonso De Mezquia et al., (2012). Also in Fig. 5b we can see a linear increase in the thermal diffusivity coefficients with pressure that is consistent with an increase of the density with pressure.

**Fig. 7** Mass diffusion  $D$  and thermal diffusivity  $\kappa$  coefficients as a function of the pressure at  $T_{\text{mean}} = 50^\circ\text{C}$  and for a temperature difference of  $\Delta T = 30^\circ\text{C}$



In Fig. 6 we report the values of mass diffusion and thermal diffusivity coefficients as a function of the mean temperature obtained for the isomassic binary mixture of decane and pentane, at  $P = 20\text{MPa}$  and for a temperature difference  $\Delta T = 30\text{ }^\circ\text{C}$ .

In Fig. 6a we can see that the mass diffusion coefficient increases with the mean temperature, which is consistent with a decrease of the viscosity of the system with the mean temperature. In Fig. 6b we can see that the thermal diffusivity coefficient decreases with the mean temperature. Again an overestimate of the reference values is detected.

In Fig. 7 we report the values of mass diffusion and thermal diffusivity coefficients as a function of the pressure obtained for the isomassic binary mixture of decane and pentane, at  $T_{\text{mean}} = 50\text{ }^\circ\text{C}$  and for a temperature difference  $\Delta T = 30\text{ }^\circ\text{C}$ . The same trends as for Fig. 5 are observed.

## Conclusions

Thermodiffusion experiments on isomassic binary mixture of decane and pentane, in the liquid phase, have been performed between  $25\text{ }^\circ\text{C}$  and  $50\text{ }^\circ\text{C}$  and for pressures from  $1\text{MPa}$  until  $20\text{MPa}$ . By means of dynamic analysis of the light scattered by concentration NE fluctuations of the binary mixture we obtained the values of the mass diffusion coefficient  $D$  at each temperature and pressure. The shadowgraph set-up and its acquisition chain enabled us to achieve a minimum delay time between two successive images of  $35\text{ms}$ . We were thus able to investigate for the first time temperature NE fluctuations, which let us model the ISF as the sum of two decreasing exponentials. This procedure allowed obtaining simultaneously the values of the thermal diffusivity coefficient  $\kappa$ . Mass diffusion coefficients  $D$  decrease with the pressure while thermal diffusivity coefficients  $\kappa$  increase with the pressure. For the investigated mixture, due to a limited intensity of the optical signal, it was not possible to obtain a reliable measurement of the Soret coefficients  $S_T$ . Therefore the obtained values of the mass diffusion coefficients  $D$  must be combined with thermodiffusion coefficients  $D_T$  measurements obtained by an independent experiment, such as thermogravitational column. The resulting values at  $50\text{ }^\circ\text{C}$  can be directly compared to measurements made in microgravity in the frame of the SCCO-SJ10 project.

**Acknowledgments** This work has been supported by the European Space Agency through the SCCO project. Support from the French space agency CNES is also acknowledged. We thank TOTAL S.A. for allowing the use of the BEST software and Research Groups (No. IT1009-16) and TERDISOMEZ (No. FIS2014-58950-C2-1-P) of MINECO.

## References

- Alonso de Mesquia, D., Bou-Ali, M.M., Larrañaga, M., Madariaga, J.A., Santamaria, C.: Determination of molecular diffusion coefficient in n-alkane binary mixtures: Empirical correlations. *J. Phys. Chem. B* **116**, 2814–2819 (2012)
- Assael, M.J., Goodwin, A.R.H., Vesovic, V., Wakeham, W.A.: Experimental thermodynamics volume IX: advances in transport properties of fluids. Royal Society of Chemistry, London (2014)
- Bou-Ali, M.M., Ahadi, A., Alonso de Mezquia, D., Galand, Q., Gebhardt, M., Khlybov, O., Köhler, W., Larrañaga, M., Legros, J.C., Lyubimova, T., Mialdun, A., Ryzhkov, I., Saghir, M.Z., Shevtsova, V., Van Vaerenbergh, S.: Benchmark values for the Soret, thermodiffusion and molecular diffusion coefficients of the ternary mixture tetralin+isobutylbenzene+n-dodecane with 0.8-0.1-0.1 mass fraction. *Eur. Phys. J. E* **38**, 30 (2015)
- Cerchiari, G., Crococolo, F., Cardinaux, F., Scheffold, F.: Quasi-real-time analysis of dynamic near field scattering data using a graphics processing unit. *Rev. Sci. Instrum.* **83**, 106101 (2012)
- Crococolo, F., Brogioli, D., Vailati, A., Giglio, M., Cannell, D.S.: Use of the dynamic Schlieren to study fluctuations during free diffusion. *App. Opt.* **45**, 2166–2173 (2006a)
- Crococolo, F., Brogioli, D., Vailati, A., Giglio, M., Cannell, D.S.: Effect of gravity on the dynamics of non equilibrium fluctuations in a free diffusion experiment. *Ann. N. Y. Acad. Sci.* **1077**, 365 (2006b)
- Crococolo, F., Brogioli, D., Vailati, A., Giglio, M., Cannell, D.S.: Non-diffusive decay of gradient driven fluctuations in a free-diffusion process. *Phys. Rev. E* **76**, 41112 (2007)
- Crococolo, F., Brogioli, D.: Quantitative Fourier analysis of schlieren masks: the transition from shadowgraph to schlieren. *App. Opt.* **50**, 3419–3427 (2011)
- Crococolo, F., Bataller, H., Scheffold, F.: A light scattering study of non equilibrium fluctuations in liquid mixtures to measure the Soret and mass diffusion coefficient. *J. Chem. Phys.* **137**, 234202 (2012)
- Crococolo, F., Bataller, H., Scheffold, F.: Static versus dynamic analysis of the influence of gravity on concentration non equilibrium fluctuations. *Eur. Phys. J. E* **37**, 105 (2014)
- De Groot, S.R., Mazur, P.: Nonequilibrium Thermodynamics. Dover, New York (1984)
- Firoozabadi, A., Ghorayeb, K., Shukla, K.: Theoretical model of thermal diffusion factors in multicomponent mixtures. *AIChE J.* **46**, 892–900 (2000)
- Galliero, G., Duguay, B., Caltagirone, J.P., Montel, F.: On thermal diffusion in binary and ternary mixtures by non-equilibrium molecular dynamics. *Phil. Mag.* **83**, 2097–2108 (2003)
- Galliero, G., Montel, F.: Understanding compositional grading in petroleum reservoirs thanks to molecular simulations, p. 121902. Society of Petroleum Engineers Paper, Amsterdam (2009)
- Galliero, G., Bataller, H., Crococolo, F., Vermorel, R., Artola, P.-A., Rousseau, B., Vesovic, V., Bou-Ali, M., Ortiz de Zárate, J.M., Xu, S., Zhang, K., Montel, F.: Impact of Thermodiffusion on the initial distribution of Species in hydrocarbon reservoirs. *Microgravity Science Technology* **28**, 79–86 (2016)
- Gebhardt, M., Köhler, W.: Soret, thermodiffusion, and mean diffusion coefficients of the ternary mixture ndodecane+isobutylbenzene+1,2,3,4 tetrahydronaphthalene. *J. Chem. Phys.* **143**, 164511 (2015)
- Georis, P., Montel, F., Van Vaerenbergh, S., Decoly, Y., Legros, J.C.: *Proc. Eur. Pet. Conf.* **1**, 57–62 (1998)
- Ghorayeb, K., Firoozabadi, A., Anraku, T.: Interpretation on the unusual fluid distribution in the Yufutsu gas-condensate field. *SPE J.* **8**, 114–123 (2003)
- Giraudet, C., Bataller, H., Crococolo, F.: High-pressure mass transport properties measured by dynamic near-field scattering of non-equilibrium fluctuations. *Eur. Phys. J. E* **37**, 107 (2014)

- Høier, L., Whitson, C.H.: Compositional grading-theory and Practice. *SPE Reserv. Eval. Eng.* **4**, 525–532 (2001)
- Kempers, L.J.T.M.: A comprehensive thermodynamic theory of the Soret effect in a multicomponent gas, liquid, or solid. *J. Chem. Phys.* **115**, 6330–6341 (2001)
- Larrañaga, M., Bou-Ali, M., Lizarraga, I., Madariaga, J.A., Santamaría, S.: Soret Coefficients of the Ternary Mixture 1,2,3,4-Tetrahydronaphthalene + Isobutylbenzene + N-Dodecane. *J. Chem. Phys.* **143**, 024202 (2015)
- Leahy-Dios, A., Bou-Ali, M.M., Platten, J.K., Firoozabadi, A.: Measurements of molecular and thermal diffusion coefficients in ternary mixtures. *J. Chem. Phys.* **122**, 234502 (2005)
- Lira-Galeana, C., Firoozabadi, A., Prausnitz, J.M.: Computation of compositional grading in hydrocarbon reservoirs. Application of continuous thermodynamics. *Fluid Phase Equilib.* **102**, 143–158 (1994)
- Montel, F., Bickert, J., Lagisquet, A., Galliero, G.: Initial state of petroleum reservoirs: a comprehensive approach. *J. Pet. Sci. Eng.* **58**, 391–402 (2007)
- Ortiz de Zárate, J.M., Sengers, J.V.: Hydrodynamic fluctuations in fluids and fluid mixtures. Elsevier, Amsterdam (2006)
- Peng, D.Y., Robinson, D.B.: A new two-constant equation of state. *Ind. Eng. Chem. Fundam.* **15**, 59–64 (1976)
- Srinivasan, S., Saghir, M.Z.: Measurements on thermodiffusion in ternary hydrocarbon mixtures at high pressure. *J. Chem. Phys.* **131**, 124508 (2009)
- Trainoff, S.P., Cannell, D.S.: Physical optics treatment of the shadow-graph. *Phys. Fluids* **14**, 1340–1363 (2002)
- Touzet, M., Galliero, G., Lazzeri, V., Saghir, M.Z., Montel, F., Legros, J.C.: Thermodiffusion: from microgravity experiments to the initial state of petroleum reservoirs. *Comptes Rendus - Mécanique* **339**, 318–323 (2011)
- VanVaerenbergh, S., Srinivasan, S., Saghir, M.Z.: Thermodiffusion in multicomponent hydrocarbon mixtures: Experimental investigations and computational analysis. *J. Chem. Phys.* **131**, 114505 (2009)
- Wu, M., Ahlers, G., Cannell, D.S.: Thermally induced fluctuations below the onset of the Rayleigh-Bénard convection. *Phys. Rev. Lett.* **75**, 17432–1746 (1995)